Cellulose (2017) 24:1611–1620
DOI 10.1007/s10570-017-1205-1

ORIGINAL PAPER

The influence of chemical treatment on the mechanical properties of windmill palm fiber

Changjie Chen · Guicui Chen · Xin Li · Hongyun Guo · Guohe Wang

Received: 11 October 2016 / Accepted: 18 January 2017 / Published online: 8 February 2017

Abstract Bleached palm fiber without lignin, alkalized palm fiber without hemicelluloses and raw windmill palm fiber were prepared. Then, the chemical composition and the mechanical properties of the windmill palm fiber were investigated. Scanning electron microscopy, Fourier transform infrared spectroscopy and Raman microscopy were employed to characterize the structure and chemical composition. A universal material tester, nanoindentation and dynamic mechanical analysis were used to study the mechanical property of these samples. According to the results, bleach treatment removed most of the silica bodies as well as the lignin, smoothed the fiber surfaces and increased the hollowness to 50%. Alkali treatment removed most of the hemicelluloses, increased the surface roughness, and reduced the hollowness to 28%. Alkalized fibers have the highest tensile strength, elongation at break and elastic modulus, with values of 119.37 ± 27.21 MPa, 30.58 ± 5.87% and 10.75 ± 4.30 GPa, respectively. The raw material without treatment has the highest stiffness, while the alkalized samples are the most flexible fibers and sensitive to temperature.

Keywords Windmill palm fiber · Chemical structure · Dynamic mechanical analysis · Mechanical properties · Nanoindentation

C. Chen · G. Chen · X. Li · H. Guo · G. Wang (✉)
College of Textile and Clothing Engineering, Soochow University, Suzhou 215006, People's Republic of China
e-mail: wangguohe@suda.edu.cn

C. Chen · G. Chen · X. Li · H. Guo · G. Wang
Nantong Textile Institute of Soochow University, Nantong 226108, People's Republic of China

G. Chen
Jiangsu Research and Development Center of the Ecological Textile Engineering and Technology, Yancheng Institute of Industry Technology, Yancheng 224005, People's Republic of China

G. Wang
Nantong Textile and Silk Industrial Technology Research Institute, Nantong 226108, People's Republic of China

Introduction

In the last decade, natural fibers, such as pineapple leaf fiber (Dos Santos et al. 2013), rice and einkorn wheat husks (Tran et al. 2014), bamboo (Liu et al. 2012), and kenaf (Dan-Mallam et al. 2013), have been studied for use in reinforcing polymers. However, there are still several potential fibers that have not yet been examined (Aldousiri et al. 2013). Windmill palms are distributed throughout the temperate and tropical zones in large numbers (Zhai et al. 2012), and their fibers are available throughout East Asia. Windmill palm fibers are obtained from the palm sheath, as the fibers are originally wrapped along the base of the palm leaf ribs (Ishak et al. 2012). Windmill palm fibers do not require any secondary processes such as water

retting or mechanical decorticating to yield the fibers, meaning they can be used directly (Ishak et al. 2012), reducing energy consumption during processing.

Due to the advantages of natural fibers as an alternative option to synthetic fibers, such as low cost, acceptable biodegradability and low density (Alajmi and Shalwan 2015; Shanmugam and Thiruchitrambalam 2013; Jawaid et al. 2013), palm trees have attracted more and more attention in recent years. The properties and commercial utilization potential of different types of palm fibers are dependent on their structural and mechanical characteristics (Zhai et al. 2012). Information on the mechanical properties of windmill palm fiber is a requirement to its further use in industrial manufacturing. An additional advantage is a potential commercial use for an item that is normally considered waste or only suitable for use in low-value products (Dehghani et al. 2013). A lack of understanding of the mechanical properties of windmill palm fibers is the present motivation for this work to determine the influence of the chemical treatment of windmill palm fibers on its mechanical properties, as few studies have investigated this issue.

This paper focuses on the mechanical properties of untreated windmill palm fibers, as well as of fibers subjected to different chemical treatments. The goal of this study is to provide background information, which will hopefully be useful in future fiber applications.

Materials

Untreated materials

The windmill palm sheath meshes used in this work were obtained from the Yuanmu Company in Hubei province, China. The windmill palm fibers (Fig. 1) were drawn off the mesh, then cleaned in running water several times and air-dried.

Bleaching treatment

The lignin from the fibers was removed by a bleaching operation using a 0.67-g/L $NaClO_2$ solution and 1.33 g/L CH_3COOH for 8 h at 80 °C (Khan et al. 2013). The fiber-to-liquor ratio was maintained at 1:50. The reaction was repeated twice or more until the fiber was completely white. Then, the fiber was washed several times using cold distilled water and dried in an oven at 60 °C for 12 h. The bleached palm fiber samples are shown in Fig. 1a.

Alkali treatment

The hemicelluloses from the fibers were removed using an alkali treatment (Wang et al. 2012, 2016). The untreated windmill palm fibers were soaked in a 6% NaOH solution in a water bath with the temperature maintained at 60 °C for 2 h and a fiber-to-liquor ratio of 1:50. Next, the fiber was mercerized in an 8 wt% NaOH solution at 60 °C for 2 h, and treated using a 10 wt% NaOH solution at 60 °C for 2 h. Then, the fibers were washed several times using cold distilled water, and dried in an oven at 60 °C for 12 h. The alkalized windmill palm fiber samples are shown in Fig. 1b.

Scanning electron microscopy (SEM) evaluation

Imaging was performed using a scanning electron microscope (SEM; S-4800, HITACHI, Japan) under a high vacuum. Dry samples were mounted on aluminum stubs and coated with gold to make the surfaces conductive. Imaging was then performed at beam accelerating voltages of 5 kV.

Diameter and hollowness test

Longitudinal optical micrographs of the treated and untreated palm fiber samples at a magnification of $\times 100$ were photographed using an Ultra depth microscope (VHX-100; Keyence, Japan). The average diameters of 300 fibers from each sample were analyzed using the Image-ProPlus 6.0 software. The SEM cross-sectional photographs of the fibers were then studied using the Image-ProPlus 6.0 software to study the hollowness. The areas of the lumen and the entire single fiber were calculated. Then, the hollowness of the fiber was determined from the area of the lumen divided by the area of the entire single fiber cross-section.

Fourier transform infrared spectroscopy (FTIR)

FTIR analysis was carried out using the KBr tableting method with a Fourier transform infrared spectrometer (Perki-Elmer; USA) run over a spectral range from 4000 to 400 cm^{-1}.

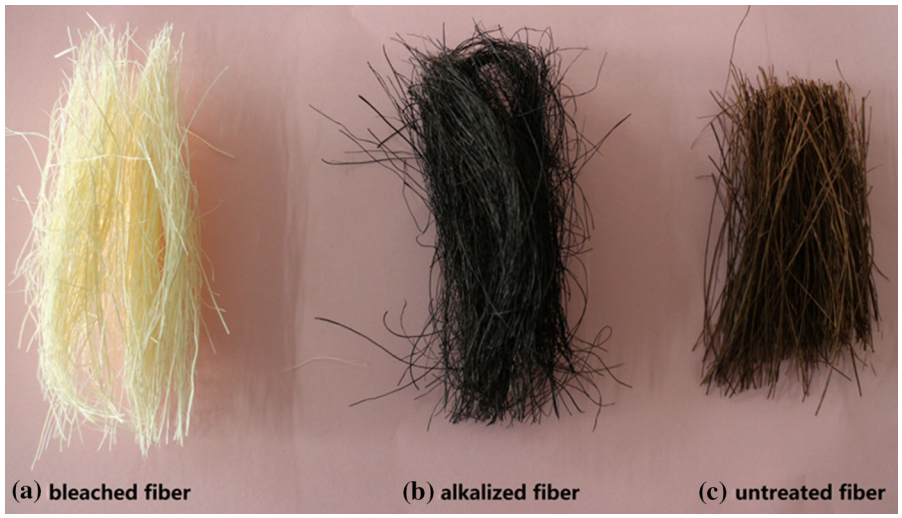

Fig. 1 **a** Bleached windmill palm fibers, **b** alkalized palm fibers and **c** untreated palm fibers

Raman microscopy

For Raman microscopy, the untreated, bleached and alkalized samples were washed with distilled water and dried naturally. The samples were then placed on a glass slide with double-faced adhesive tape. The spectra were acquired using a Micro-Raman Spectrometer (Labram Xplora, Horibajy, France) using a linear-polarized 532-nm laser excitation power of 25 mW.

Tensile property test

Tensile testing for the windmill palm fibers was performed according to the ASTM C1557 standard. According to the standard guideline, three different gauge lengths (20, 30, and 40 mm) for each series of windmill palms were used to determine their tensile properties and system compliance. A total of 45 samples were fabricated for each type; thus, 15 specimens were made for each gauge length. Tensile tests were conducted in a universal material tester (Instron 5967, USA) using a 500-N load cell with a 0.05-mm/s cross-head speed.

The tensile modulus was obtained during experimentation and used to calculate the system compliance from Eq. (1):

$$\frac{\Delta L}{F} = \frac{L_0}{AE} + C_s \tag{1}$$

where ΔL is the total measured displacement, F is the applied force, C_S is the system compliance, L_0 is the gage length, A is the cross-sectional area of the fiber and E is the tensile modulus. Thus, a linear representation of $\Delta L/F$ as a function of L_0/A will yield a straight line slope $1/E$ and intercept the system compliance C_S (Gowthaman et al. 2017; Mahjoub et al. 2014; Paiva et al. 2007). To calculate the cross-sectional area and the strength of the tested palm fibers, an image of the cross-section was measured using a digital microscope (VHX-100; Keyence). An image-processing software (Image-ProPlus 5.0) was used to measure the cross-sectional area.

Nanoindentation test

Each sample was embedded in epoxy resin for nanoindentation testing. Embedded windmill palm fiber samples were polished using a grinder to prepare the surfaces. Nanoindentation was performed using an instrumented micro/nanoindentation/scratch system (NHT2/MCT; Switzerland) with a Vickers tip along the depth of the cross-section. In total, 12 indentations were conducted at different positions for each sample. The indentation tests were performed in force-controlled mode, where the indenter tip was loaded to a peak force of 0.5 mN at a loading rate of 1 mN/s, held at a constant load for 10 s, and unloaded at a rate of 1 mN/s. The hardness (H) and the elastic modulus (Er)

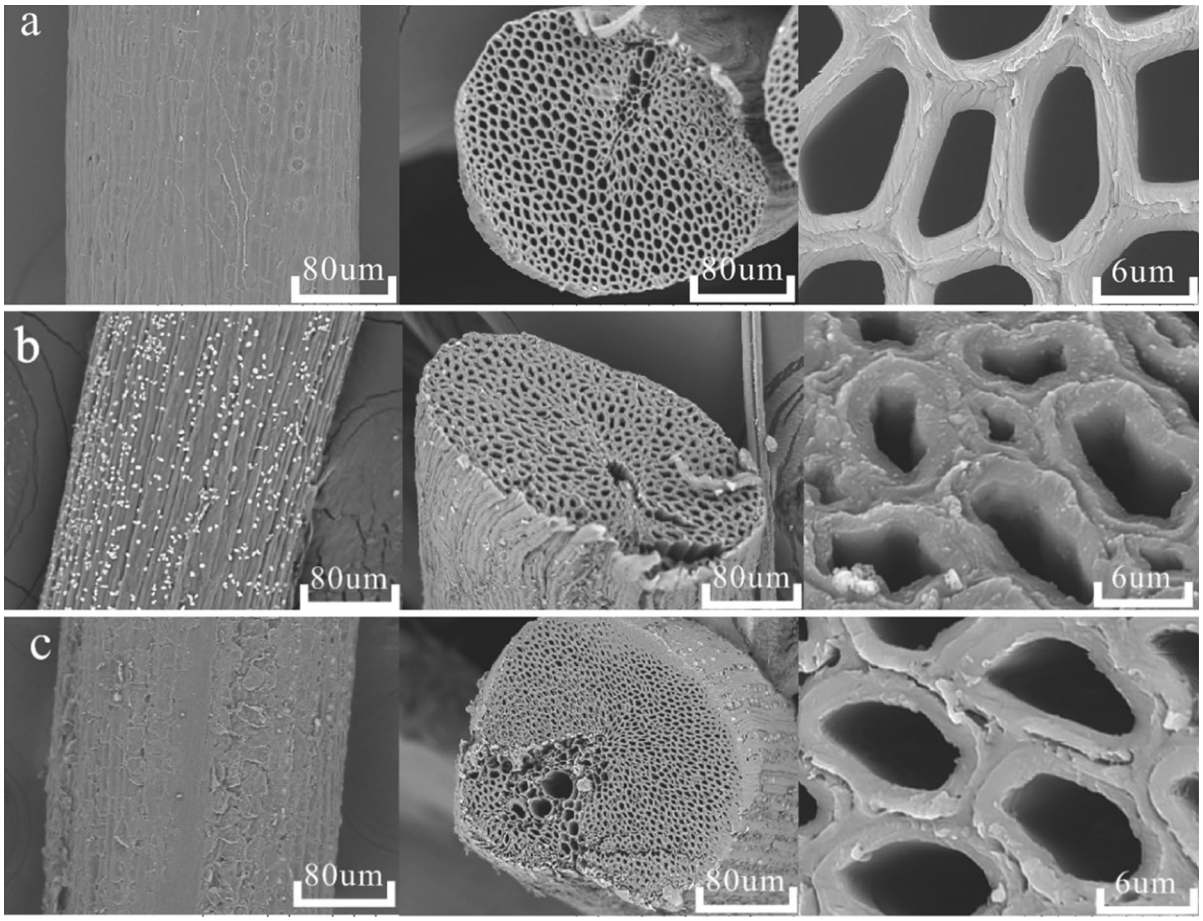

Fig. 2 SEM images of **a** bleached windmill parm fiber, **b** alkalized palm fiber, and **c** untreated palm fiber

were obtained from the curve using the method developed by Oliver and Pharr (1992, 2004).

Dynamic mechanical thermal analysis (DMTA)

Scanning electron microscopy (TM3030; Japan) was used to characterize the dimensions of the windmill palm fibers. All the DMTA tests were performed on a Q800-type tester (TA Instruments, USA) with the following input parameters: dynamic force of 0.5 cN, frequency of 1 Hz, heating ratio of 10 °C/min and temperature range of 35–235 °C. Three specimens were analyzed for each sample. The analysis enabled the determination of the storage modulus (E') from the in-phase response, the loss modulus (E") from the out-of-phase response, and the magnitude of tan δ.

Results and discussion

Morphological properties of the windmill palm fibers

Changes in the surface morphology of the windmill palm fibers after different treatments were determined from the SEM (Fig. 2). Silica-bodies attach themselves to circular craters, which are spread relatively uniformly over the fiber surface. After the bleaching treatment, most of these silica-bodies are removed. As a result, a relatively smooth fiber surface and a thin diameter (225.24 ± 97.77 μm) are observed. A lumen clearly exists in the middle of the fiber after bleaching, and the degree of hollowness is approximately 50%, indicative of a slight increase.

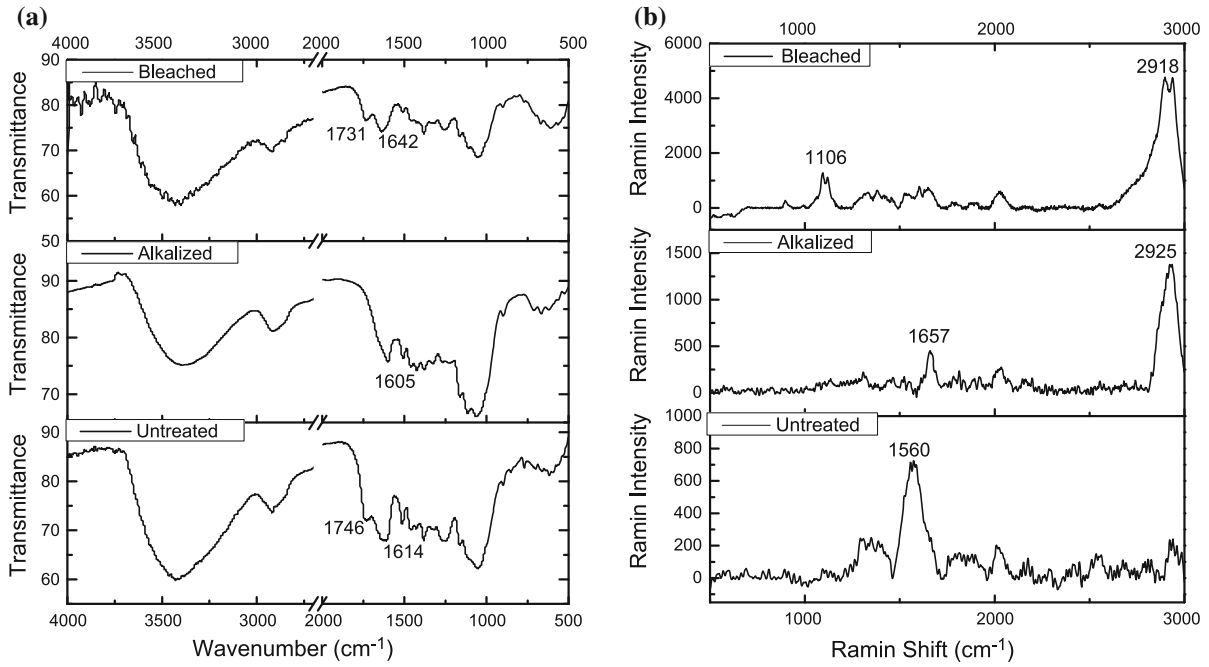

Fig. 3 **a** FTIR and **b** Raman spectra of windmill palm fiber

As shown in Fig. 2b, the alkali treatment increases the surface roughness and causes more separation in the cellulose fibers exposed on the fiber surface. This phenomenon has been observed in other studies of the morphology of several alkalized natural fibers (Mahjoub et al. 2014; Chowdhury et al. 2013; Khan et al. 2013; Akil et al. 2011). A mound of droplets containing lignin were observed on the alkalized windmill palm fiber surface. In an aqueous environment, hydrophobic lignins minimize their surface area contacting water, causing them to coalesce and form spheres (Ma et al. 2014; Donohoe et al. 2008). These lignin droplets are observed on the cross-section. Alkali treatment causes swelling in the fiber cell walls. As a result, the degree of hollowness decreased greatly, from 46 to 28% for the untreated windmill palm fiber. The alkalized palm fiber has the smallest diameter, of approximately 138.38 ± 63.02 μm, whereas the average diameter of the untreated windmill palm fiber is approximately 308.77 ± 101.79 μm.

Effect of treatment on chemical composition of windmill palm fiber

Raman and infrared spectroscopy can provide "complementary" information on the molecular vibrations (Gierlinger et al. 2008). As a result, the spectrums from Raman and infrared spectroscopy are shown in Fig. 3.

The FTIR spectra of the windmill palm fiber are as shown in Fig. 3a. Prominent peaks at 1731 and 1745 cm^{-1} are observed in the spectra of the raw windmill palm fiber and the fiber after bleaching. However, this peak vanishes in the alkalized samples. The peak at approximately 1730–1750 cm^{-1} was associated with the presence of the ester linkages of the carboxylic groups of the ferulic and *p*-coumeric acids of the hemicellulose (Goh et al. 2016; Sain and Panthapulakkal 2006). Additionally, the peak formed at 1636 cm^{-1} confirms the existence of the hemicelluloses (Binoj et al. 2016). All these results substantiated that most of the hemicelluloses were effectively removed after the alkali treatments.

The Raman spectra of the windmill palm fiber are as shown in Fig. 2b. The peaks at 1080 and 1150 cm^{-1} correspond mainly to C–C ringbreathing and C–O–C stretching vibrations from carbohydrates (Edwards et al. 1997; Kacuráková et al. 1999; Gierlinger et al. 2008). There are no distinct absorption bands in this region because the alkali treatment releases most of the hemicellulose. The broad "band" between 1460 and 1700 cm^{-1} is assigned to the lignin and exhibits a

higher intensity in the spectrum from the raw materials (Ma et al. 2014). The disappearance of the lignin peak in the bleached samples indicates that it was removed after the bleach treatment. The most prominent bands are found in the region between 2800 and 3000 cm^{-1} and are assigned to the C–CH_3, O–CH_3 and CH_2 stretching modes (Gierlinger et al. 2008) deriving from the cellulose in the windmill palm fiber wall (Gierlinger and Schwanninger 2007).

Tensile property of windmill palm fibers

The system compliance method, which is suitable for the indirect measurement of elongation according to ASTM C1557, was used to analyze the tensile test results for the bleached, alkalized and untreated windmill palm fibers. A graphical representation of Eq. (1) for the bleached windmill palm fibers tested using different gauge lengths is shown in Fig. 4. The constant slope of the straight line is $1/E_k$, whereas the y intercept is the system compliance (Cs).

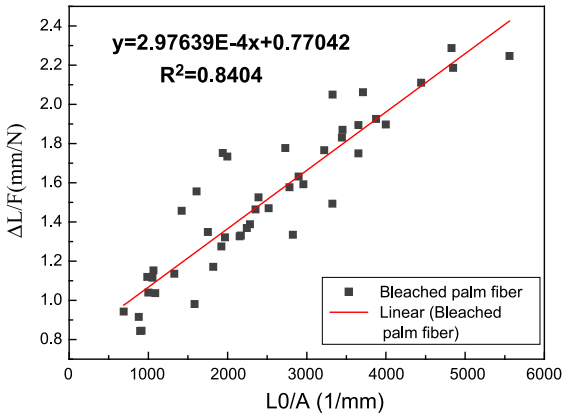

Fig. 4 System compliance method for bleached windmill palm fibers

The tensile properties of the untreated and treated windmill palm fibers are shown in Table 1. From this, we can see that the tensile properties of the fibers were affected by their chemical treatment. Hemicellulose is a form of random, amorphous branched or nonlinear structures with little strength (Summerscales et al. 2010). The release of the hemicellulose increases the mechanical properties. The tensile strength and the E_k of alkalized fibers almost free of hemicelluloses are the highest, at 392.13 ± 101.36 and 7799.70 MPa, respectively. The tensile strengths of the untreated and bleached fibers are 302.62 ± 105.02 and 324.96 ± 84.33 MPa, respectively, whereas the E_k values are 2724.58 and 3359.76 MPa, respectively. After the bleach or alkali treatment, most of the lignin or hemicellulose in the windmill palm fiber is released, causing the elongation at break to decrease.

The elongation at break of different windmill palm fibers is shown in Fig. 5. The untreated palm fiber has the highest elongation of 35.788 ± 4.39%, at the test length of 2 mm, while the elongation decreases to 26.58 ± 5.45% at the test length of 4 mm, while the average elongation of untreated windmill palm fiber is 30.88 ± 5.77%. Untreated windmill palm fiber exhibits an excellent strain property because of its high microfibril angle, hierarchical composite structure and delamination within and between hollow fiber cells during the loading process (Zhang et al. 2015). The fiber elongation decreases when the test length increases, following the probability of breakage theory (Tran et al. 2015), except for the bleached fiber at 4 mm. Therefore, the effect of test length on the elongation of the bleached and alkalized fibers is smaller. The average elongations of the bleached and

Table 1 Tensile properties of windmill palm fiber by using of system compliance method

Samples	Line equation	R^2	System compliance (Cs) of machine (mm/N)	E_k (tensile modulus) (MPa)	Tensile strength value (MPa)			Elongation value (%)		
					Mean	SD	CV	Mean	SD	CV
Bleached	$\frac{\Delta L}{F} = 2.9764 \times 10^{-4} \frac{L_0}{A} + 0.77042$	0.84	0.77042	3359.76	324.96	84.33	25.95	24.15	6.55	27.13
Alkalized	$\frac{\Delta L}{F} = 1.2821 \times 10^{-4} \frac{L_0}{A} + 0.76261$	0.76	0.76261	7799.70	392.13	101.36	25.85	23.60	6.33	26.82
Untreated	$\frac{\Delta L}{F} = 3.67092 \times 10^{-4} \frac{L_0}{A} + 0.47624$	0.72	0.47624	2724.58	302.62	105.02	34.70	30.88	5.77	18.70

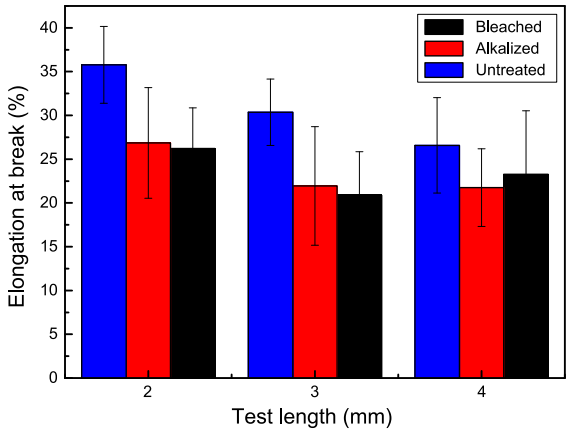

Fig. 5 Elongation at break of chemical-treated windmill palm fibers at different test length

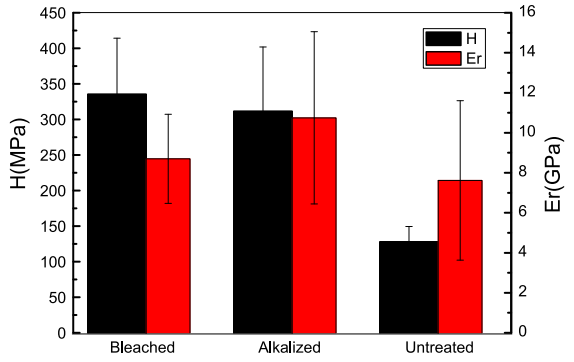

Fig. 6 Hardness (*H*) and indentation modulus (Er) of the secondary cell wall of windmill palm fibers

alkalized fibers are nearly the same at 24.15 ± 6.55 and 23.60 ± 6.33%, respectively. The high elongation at break percentage of windmill palm has the potential advantage to rectify weaknesses possessed by brittle composite materials. The unique mechanical properties make the material a good natural resource for enhancing the composite materials (Zhai et al. 2012).

The strain is more dependent on, and increases with, the micro-fibril angle (Yang et al. 2016). The decrease in the elongation at break may indicate that the chemical treatment increases the micro-fibril angle. Overall, the tensile strength of the windmill palm fibers is equal to that of surge palm fibers (100–450 MPa) (Sahari et al. 2012) or coir fibers (160–300 MPa) (Tran et al. 2015), but lower than kenaf fibers (200–300 MPa) (Ochi 2008).

Nanoindentation measurement of the windmill palm fiber

Nanoindentation, which is otherwise known as instrumented or depth-sensing indentation (Oliver and Pharr 1992, 2004; Eder et al. 2013; Gale and Achuthan 2014; N'Jock et al. 2015), is a well-established technique to characterize the mechanical properties of materials at very small length scales. From the stress–strain curve obtained by the nanoindentation test, two important parameters, the hardness (*H*) and elastic modulus (Er), which is also known as the indentation modulus, can be determined. Figure 6 shows the values obtained for the nanoindentation modulus and hardnesses of three different samples. The hardness of the bleached sample which has had its lignin removed (335.26 ± 78.92 MPa) is similar to the alkalized sample (311.37 ± 90.51 MPa) and harder than the untreated sample (127.38 ± 22.10 MPa). The alkalized sample without hemicelluloses has the highest Er of 10.75 ± 4.30 GPa.

Table 2 Comparison of mechanical properties of hardwoods, softwoods, lyocell fibers and bamboo that measured by nanoindentation

Species		Hardness (MPa)	Elastic modulus (GPa)
Hardwoods	Poplar, Iroko, Alder birch, Manchuria ash, Asian white birch, Red oak, White oak, Mongolian oak, Kwila, Keranji	400–560	14.2–35.4
Softwoods	Loblolly pine, Spruce	340–530	14.2–18
Crops	Cotton stalk, Cassava stalk, Soybean stalk, Rice straw, Wheat straw	480–850	16.3–20.8
Lyocell fiber		330–440	11.5–13.2
Bamboo		290–507	4.5–8.6

To further understand the mechanical characteristics of the windmill palm fibers, the results have been compared to those for ten kinds of hardwoods (Wu et al. 2009), two kinds of softwoods, five kinds of crops, and lyocell fibers, especially bamboo (Wu et al. 2010), as shown in Table 2. The indentation modulus and hardness of three different types of windmill palm

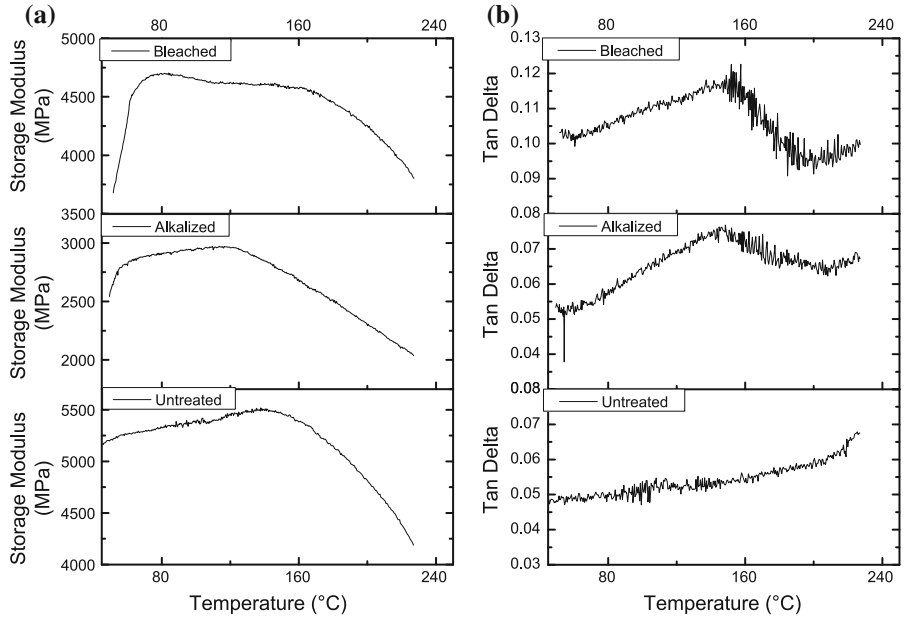

Fig. 7 **a** E'–T and **b** tan δ–T curves of different windmill palm fibers

fiber cell walls is slightly lower than that of the hardwood, softwood, and crops and is similar to bamboo and lyocell fibers. In general, they are within the same order of magnitude.

Thermo-mechanical properties of windmill palm fibers

DMTA, which is generally recognized as being sensitive to molecular motion, is used to measure the stiffness and damping of a structure (Kim et al. 2013; Waldron and Harwood 2011). Figure 7 show the dependence of the storage modulus (E') and tan δ on temperature (T) for the windmill palm fibers.

The storage modulus represents the ability of any material to store mechanical energy and resist deformation, and is related to the elastic performance of a material and is similar, though not identical, to the Young's modulus (Waldron and Harwood 2011; Fabiyi and Ogunleye 2015). The storage modulus value of the untreated windmill palm fibers was found to be approximately 5500 MPa, which is higher than the others. After the bleaching treatment, the storage modulus decreases to 4700 MPa, whereas the storage modulus of the alkalized fibers is approximately 3000 MPa. This indicates that the raw material without being subjected to any treatment has the highest stiffness, whereas the alkalized samples are the most flexible (Waldron and Harwood 2011).

The tan δ of the untreated windmill palm fibers increases with temperature. The temperature corresponding to the tan δ peak for the bleached and alkalized samples are approximately 153 and 146 °C, respectively. The lower temperature at the tan δ peak suggests that it is easier to achieve maximum viscosity. This may indicate that, after the alkali treatment, the windmill palm fibers are most sensitive to the temperature. In contrast, the tan δ peak for the untreated windmill palm fibers corresponds to the highest heating temperature, indicating that the raw materials are least sensitive to temperature and exhibit excellent thermal stability (Xia et al. 2016).

Conclusion

In this work, a bleaching treatment was used to remove most of the silica-bodies and provide relatively smooth fiber surfaces. The degree of hollowness of the bleached fibers almost without lignin is approximately 50%, which is slightly higher than the 46% observed in the raw materials. The alkali treatment removed almost all of the hemicelluloses, increased the surface roughness and exposed more cellulose. The alkalized fibers

with a degree of hollowness of 28% are surrounded by a large number of lignin droplets.

The alkalized fibers have the highest tensile strength and modulus of 392.13 ± 101.36 and 7799.70 MPa, respectively. The untreated palm fibers have the highest average elongation at break of $30.88 \pm 5.77\%$.

The hardness of the bleached fibers without lignin is similar to that of the alkalized sample and harder than the untreated sample. The alkalized sample without hemicelluloses has the highest elastic modulus Er (10.75 ± 4.30 GPa). The raw material without treatment has the highest stiffness with a storage modulus of approximately 5500 MPa, whereas the alkalized samples are the most flexible fibers and are sensitive to temperature.

Acknowledgments This work was funded by the Priority Academic Program Development of Jiangsu Higher Education Institutions, China (No. 37 [2014]); and the Jiangsu Province Special Project, China (No. BY2014083).

References

Akil HM, Omar MF, Mazuki AAM, Safiee S, Ishak ZAM, Abu Bakar A (2011) Kenaf fiber reinforced composites: a review. Mater Des 32(8):4107–4121

Alajmi M, Shalwan A (2015) Correlation between mechanical properties with specific wear rate and the coefficient of friction of graphite/epoxy composites. Materials 8:4162–4175

Aldousiri B, Alajmi M, Shalwan A (2013) Mechanical properties of palm fiber reinforced recycled HDPE. Adv Mater Sci Eng 2013:511–516

Binoj JS, Raj RE, Sreenivasan VS, Thusnavis GR (2016) Morphological, physical, mechanical, chemical and thermal characterization of sustainable Indian areca fruit husk fibers (*Areca Catechu* L.) as potential alternate for hazardous synthetic fibers. J Bionic Eng 13:156–165

Chowdhury MNK, Beg MDH, Khan MR, Mina MF (2013) Modification of oil palm empty fruit bunch fibers by nanoparticle impregnation and alkali treatment. Cellulose 20(3):1477–1490

Dan-Mallam Y, Abdullah MZ, Yosuff PSM (2013) Impact strength, microstructure, and water absorption properties of kenaf/polyethylene terephthalate (PET) fiber-reinforced polyoxymethylene (POM) hybrid composites. J Mater Res 28(16):2142–2146

Dehghani A, Ardekani SM, Al-Maadeed MA, Hassan A, Wahit MU (2013) Mechanical and thermal properties of date palm leaf fiber reinforced recycled poly (ethylene terephthalate) composites. Mater Des 52:841–848

Donohoe BS, Decker SR, Tucker MP, Himmel ME, Vinzant TB (2008) Visualizing lignin coalescence and migration through maizecell walls following thermochemical pretreatment. Biotechnol Bioeng 101(5):913–925

Dos Santos RM, Neto WPF, Silvério HA, Martins DF, Dantas NO, Pasquini D (2013) Cellulose nanocrystals from pineapple leaf, a new approach for the reuse of this agro-waste. Ind Crops Prod 50:707–714

Eder M, Arnould O, Dunlop JW, Hornatowska J, Salmén L (2013) Experimental micromechanical characterisation of wood cell walls. Wood Sci Technol 47(1):163–182

Edwards HGM, Farwell DW, Webster D (1997) FT Raman micros-copy of untreated natural plant Wbres. Spectrochim Acta A 53:2383–2392

Fabiyi JS, Ogunleye BM (2015) Mid-infrared spectroscopy and dynamic analysis of heat-treated obeche (*Triplochiton scleroxylon*) wood. Maderas Cienc Technol 17:5–16

Gale JD, Achuthan A (2014) The effect of work-hardening and pile-up on nanoindentation measurements. J Mater Sci 49:5066–5075

Gierlinger N, Schwanninger M (2007) The potential of Raman microscopy and Raman imaging in plant research. Spectrosc Int J 21:69–89

Gierlinger N, Sapei L, Paris O (2008) Insights into the chemical composition of Equisetum hyemale by high resolution Raman imaging. Planta 227:969–980

Goh KY, Ching YC, Chuah CH, Abdullah LC, Liou NS (2016) Individualization of microfibrillated celluloses from oil palm empty fruit bunch: comparative studies between acid hydrolysis and ammonium persulfate oxidation. Cellulose 23:379–390

Gowthaman S, Sankar CG, Chandrakumar P (2017) Evaluation of tensile properties of natural silk and coir fibers. In: Bajpai RP, Chandrasekhar U (eds) Innovative design and development practices in aerospace and automotive engineering. Springer, Singapore, pp 393–399

Ishak MR, Sapuan SM, Leman Z, Rahman MZA, Anwar UMK (2012) Characterization of sugar palm (Arenga pinnata) fibres. J Therm Anal Calorim 109:981–989

Jawaid M, Khalil H, Hassan A, Dungani R, Hadiyane A (2013) Effect of jute fibre loading on tensile and dynamic mechanical properties of oil palm epoxy composites. Compos Part B 45:619–624

Kacuráková M, Wellner N, Ebringerova A, Hromádková Z, Wilson RH, Belton PS (1999) Characterisation of xylan-type polysaccha-rides and associated cell wall components by FT-IR and FT-Ra-man spectroscopies. Food Hydrocoll 13:35–41

Khan GMA, Shams MSA, Kabir MR, Gafur MA, Terano M, Alam MS (2013) Influence of chemical treatment on the properties of banana stem fiber and banana stem fiber/coir hybrid fiber reinforced maleic anhydride grafted polypropylene/low-density polyethylene composites. J Appl Polym Sci 128:1020–1029

Kim JW, Park S, Harper DP, Rials TG (2013) Structure and thermomechanical properties of stretched cellulose films. J Appl Polym Sci 128:181–187

Liu D, Song J, Anderson DP, Chang PR, Hua Y (2012) Bamboo fiber and its reinforced composites: structure and properties. Cellulose 19(5):1449–1480

Ma J, Zhang X, Zhou X, Xu F (2014) Revealing the changes in topochemical characteristics of poplar cell wall during hydrothermal pretreatment. Bioenerg Res 7:1358–1368

Mahjoub R, Jamaludin MY, Abdul Rahman MS, Hashemi SH (2014) Tensile properties of kenaf fiber due to various

conditions of chemical fiber surface modifications. Constr Build Mater 55:103–113

N'Jock MY, Chicot D, Ndjaka JM, Lesage J, Decoopman X, Roudet E, Mejias A (2015) A criterion to identify sinking-in and piling-up in indentation of materials. Int J Mech Sci 90:145–150

Ochi S (2008) Mechanical properties of kenaf fibers and kenaf/PLA composites. Mech Mater 40(4–5):446–452

Oliver WC, Pharr GM (1992) An improved technique for determining hardness and elastic modulus using load and displacement sensing indentation experiments. J Mater Res 7(06):1564–1583

Oliver WC, Pharr GM (2004) Measurement of hardness and elastic modulus by instrumented indentation: advances in understanding and refinements to methodology. J Mater Res 19(01):3–20

Paiva MC, Ammar I, Campos AR, Cheikh RB, Cunha AM (2007) Alfa fibres: mechanical, morphological and interfacial characterization. Compos Sci Technol 67(6):1132–1138

Sahari J, Sapuan SM, Ismarrubie ZN, Rahman MZA (2012) Physical and chemical properties of different morphological parts of sugar palm fibres. Fibres Text East Eur 20:21–24

Sain M, Panthapulakkal S (2006) Bioprocess preparation of wheat straw fibers and their characterization. Ind Crops Prod 23(1):1–8

Shanmugam D, Thiruchitrambalam M (2013) Static and dynamic mechanical properties of alkali treated unidirectional continuous palmyra palm leaf stalk fiber/jute fiber reinforced hybrid polyester composites. Mater Des 50:533–542

Summerscales J, Dissanayake NP, Virk AS, Hall W (2010) A review of bast fibres and their composites. Part 1—fibres as reinforcements. Compos A 41(10):1329–1335

Tran TPT, Bénézet JC, Bergeret A (2014) Rice and Einkorn wheat husks reinforced poly (lactic acid) (PLA) biocomposites: effects of alkaline and silane surface treatments of husks. Ind Crops Prod 58:111–124

Tran LQN, Minh TN, Fuentes CA, Chi TT, van Vuure AW, Verpoest I (2015) Investigation of microstructure and tensile properties of porous natural coir fiber for use in composite materials. Ind Crops Prod 65:437–445

Waldron D, Harwood J (2011) A preliminary investigation into the influence of chemical composition on the dynamic mechanical properties of flax (Linum usitattisimum) Straw. J Nat Fibers 8:126–142

Wang CG, Jiang ZH, Fei BH, Yu Y, Zhang SY (2012) Effects of chemical components on longitudinal MOE and hardness of wood cell wall. J Beijing For Univ 34(3):107–110

Wang S, Zhang TH, Li JL, Fang LM, Liu XX, Guo M (2016) Exploration of the origin of the UV absorption performance of windmill palm fiber. Bioresources 11:2607–2616

Wu Y, Wang S, Zhou D, Xing C, Zhang Y (2009) Use of nanoindentation and silviscan to determine the mechanical properties of 10 hardwood species. Wood Fiber Sci 41(1):64–73

Wu Y, Wang S, Zhou D, Xing C, Zhang Y, Cai Z (2010) Evaluation of elastic modulus and hardness of crop stalks cell walls by nano-indentation. Bioresour Technol 101(8):2867–2871

Xia ZG, Yao CE, Zhou JH, Ye WX, Xu WL (2016) Comparative study of cotton, ramie and wool fiber bundles' thermal and dynamic mechanical thermal properties. Text Res J 86:856–867

Yang X, Liu XG, Shang LL, Ma JF, Tian GL, Yang SM (2016) Variation of tensile properties of single fibres of dendrocalamus farinosus bamboo. Bioresources 11:1609–1619

Zhai SC, Li DG, Pan B, Sugiyama J, Itoh T (2012) Tensile strength of windmill palm (*Trachycarpus fortunei*) fiber bundles and its structural implications. J Mater Sci 47:949–959

Zhang TH, Guo M, Cheng L, Li X (2015) Investigations on the structure and properties of palm leaf sheath fiber. Cellulose 22(2):1039–1051